APPENDIX PA

ATTACHMENT PORSURF

This page intentionally left blank

Table of Contents

List of Figures

This page intentionally left blank

PORSURF.1 INTRODUCTION

Creep closure of the excavation and the presence of either brine or gas in the waste disposal region both influence time-dependent changes in void volume in the waste disposal area. As a consequence, these processes influence two-phase fluid flow of brine and gases through the waste and its capacity for storing fluids. For the performance assessment (PA), a porosity surface method is used to indirectly couple mechanical closure and gas generation with two-phase fluid flow calculations implemented in the BRAGFLO code (Appendix PA, Section PA 4.2). The porosity surface approach is used because current codes are not capable of fully coupling creep closure, waste consolidation, brine availability, and gas production and migration with computational efficiency. The porosity surface method incorporates the results of closure calculations obtained from the SANTOS code, a quasistatic, large deformation finite-element structural analysis code (Stone 1997). The adequacy of the method is documented in Freeze (1996), who concludes that the approximation is valid so long as the rate of room pressurization in final calculations is bounded by the room pressurization history that was used to develop the porosity surface.

The porosity surface used in the CRA-2004 PA is the same surface that was used for the CCA PA. Consequently, the models and parameters used to calculate this surface are unchanged from the CCA PA. For information on the porosity surface used in the CCA PA, see CCA Appendix PORSURF.

A separate analysis considered the potential effects on repository performance of uncertainty in the porosity surface (Appendix PA, Attachment MASS, Section MASS.2.0). Uncertainty in the porosity surface can arise from heterogeneity in the rigidity of waste packages, and from uncertain spatial arrangement of waste in the repository. The analysis considered four porosity surfaces, including the surface from the CCA, which represented various bounding combinations of waste package rigidity and waste initial porosity. The analysis concluded that uncertainty in porosity surface did not have significant effects on repository performance, and recommended the continued use of the CCA porosity surface in PA.

PORSURF.2 CREEP CLOSURE METHOD

Creep closure is accounted for in BRAGFLO by changing the porosity of the waste disposal area according to a table of porosity values, termed the porosity surface. The porosity surface is generated using the nonlinear finite element code, SANTOS. Disposal room porosity is calculated over time, varying the rate of gas generation and the gas production potential, to construct a three-dimensional porosity surface representing changes in porosity as a function of pressure and time over the 10,000-year simulation period.

The completed porosity surface is compiled in tabular form and is used in the solution of the gas and brine mass balance equations presented in Appendix PA Section PA-4.2.1. Porosity is interpolated from the porosity surface corresponding to the calculated gas pressure at time level t_n. The porosity surface is then accessed iteratively for the remainder of the simulation at the end of each BRAGFLO time step t_{n+1}. The closure data provided by SANTOS can be viewed as a series of surfaces, with any gas generation history computed by BRAGFLO constrained to fall on this surface. Various techniques described in Freeze et al. (1995) were used to check the validity of this approach, and it was found to be a reasonable representation of the behavior observed in the complex models.

In SANTOS, gas pressure in the disposal room is computed from the ideal gas law by the following relationship:

$$p_g = \frac{NRT}{V},$$

where N is the mass of gas in moles at a given time, R is the universal gas constant (8.23 m^3 Pa/ mole °K), T is the absolute temperature in degrees Kelvin (constant at 300° K), and V is the current free volume of the room. The mass of gas is computed as

$$N = r(t, f) \times Ndrums \times t ,$$

where $r(t, f)$ is the gas generation rate (moles/drum/yr) at time t for the scaling factor f and Ndrums is the number of drums of waste in the room (6804 drums per room). The base gas generation rate in SANTOS is

$$r(t,1) = \begin{cases} 2 \text{ mol/drum/yr} & 0 \le t \le 550 \text{ yr} \\ 1 \text{ mol/drum/yr} & 550 \text{ yr} \le t \le 1050 \text{ yr} \\ 0 \text{ mol/drum/yr} & 1050 \text{ yr} \le t \end{cases} .$$

The base gas generation rate $r(t,1)$ is representative of relatively high gas production rates from both microbial degradation of cellulosic, plastic and rubber materials and from anoxic corrosion of Fe-base metals (Butcher 1997b). To provide a range of SANTOS results that spans the possible range of pressure computed by BRAGFLO, the gas generation rate is varied by the scaling factor f. Thirteen values of f are used to construct the porosity surface: f = 0.0, 0.025, 0.05, 0.1, 0.2, 0.4, 0.5, 0.6, 0.8, 1.0, 1.2, 1.6, and 2.0. The condition of f = 0 represents the state of the repository when no gas is produced; f = 2 represents twice the base gas generation rate. The gas generation rate for each case is computed by

$$r(t, f) = f \times r(t,1).$$

The gas generation potentials and rates used in SANTOS are not the same as are used in BRAGFLO, the PA model for two-phase flow in the repository (see Appendix PA, Section PA-4.2). In SANTOS, gas generation is included to introduce a range of values for gas pressure during room closure, thereby capturing the effects of gas pressure on room closure; the use of the scaling factor f ensures that SANTOS results span a wide range of possible gas generation rates and potentials. In contrast, the BRAGFLO code computes the amount of gas generated at each time step, using a stoichiometric model that accounts for the inventory of gas-generation substrates, the saturation of the waste material, and the uncertain parameters in the gas generation model.

PORSURF.3 CONCEPTUAL MODEL FOR POROSITY SURFACE

The ability of salt to deform with time, eliminate voids, and create an impermeable salt barrier around the waste was one of the principal reasons for locating the WIPP repository in a bedded salt formation. The creep closure process is a complex and interdependent series of events starting after a region within the repository is excavated. Immediately upon excavation, the equilibrium state of the rock surrounding the repository is disturbed, and the rock begins to deform and return to equilibrium. Eventually, at equilibrium, deformation ceases, and the waste region has undergone as much compaction as is possible under the prevailing lithostatic stress field.

Creep closure of the excavation begins immediately and causes the volume of the cavity to become smaller. If the room were empty, rather than partially filled with waste, closure would proceed to the point where the void volume created by the excavation would be eliminated and the surrounding halite would return to its undisturbed, uniform stress state. In a waste-filled room, the rock will contact the waste and the rate of closure will decrease as the waste compacts and stiffens; eventually, closure will cease when the waste can take the full overburden load without further deformation. Initially, unconsolidated waste can support only small loads, but as the room continues to close after contact with the waste, the waste will consolidate and support a greater portion of the weight of the overburden. Consolidation will continue until mechanical equilibrium is reached.

The presence of gas in the room will retard the closure process due to the build-up of pressure. As the waste consolidates, pore volume is reduced and pore pressure increases (using the ideal gas law). In this process, the waste can be considered to be a skeleton structure immersed in a pore fluid (the gas). As the pore pressure increases, less of the weight of the overburden is carried by the skeleton, and more support is provided by the gas. If the gas pressure increases to lithostatic pressure, the pore pressure alone is sufficient to support the overburden.

PORSURF.4 SANTOS NUMERICAL ANALYSES

Computation of repository creep closure is a particularly challenging structural engineering problem, because the rock surrounding the repository continually deforms with time until equilibrium is reached. Not only is the deformation of the salt inelastic, but it also involves larger deformations than are customarily addressed with conventional structural deformation codes. In addition, the formation surrounding the repository is not homogeneous in composition, containing various parting planes and interbeds with different properties than the salt.

Deformation of the waste is also nonlinear, with large strains, and the response of a waste-filled room is complicated by the presence of gas. These complex characteristics of the materials comprising the repository and its surroundings require the use of highly specialized constitutive models. Appropriate models have been built into the SANTOS code over a number of years. Principal components of the SANTOS model include:

1. Disposal Room Configuration and Idealized Stratigraphy. Disposal room dimensions, computational configuration, and idealized stratigraphy are defined in Attachment 1 to

CCA Appendix PORSURF. The idealized stratigraphy is reproduced in Figure PORSURF-1 of this Attachment.

2. Discretized Finite Element Model. A two-dimensional plane strain model, as shown in Figure PORSURF-2, is used for the SANTOS analyses. The discretized model represents the room as one of an infinite number of rooms located at the repository horizon. The model contains 1,680 quadrilateral uniform-strain elements and 1,805 nodal points. Contact surfaces between the stored waste and the surfaces of the room are addressed. Justification for this model and additional detail on initial and boundary conditions is provided in Attachment 1 to CCA Appendix PORSURF.

3. Geomechanical Model. Mechanical material response models and their corresponding property values are assigned to each region of the configuration. These models include:

   A. a combined transient-secondary creep constitutive model for clean and argillaceous halite;

   B. an inelastic constitutive model for anhydrite; and

   C. a volumetric plasticity model for waste.

   Material properties are provided in CCA Appendix PORSURF.

The results of the SANTOS calculations are illustrated in Figures PORSURF-3 and PORSURF-4. Figure PORSURF-3 shows disposal room porosity as a function of time for various values of the gas generation scaling factor f. Figure PORSURF-4 shows disposal room pressure as a function of time for various values of f. When f = 0, no gas is present in the disposal room, thus, disposal room pressure is identically zero for all times, and this pressure curve is omitted from Figure PORSURF-4.

PORSURF.5 IMPLEMENTATION OF POROSITY SURFACE IN BRAGFLO

As outlined in Section PORSURF.3, the SANTOS program is used to determine time-dependent porosities and pressures in the repository under different rates of gas generation determined by the scaling factor f. Calculation with each value of f results in the porosity and pressure curves in Figures PORSURF-3 and PORSURF-4.

The porosities calculated by SANTOS are defined relative to a dynamically changing excavated volume. In contrast, BRAGFLO assumes a fixed excavated volume, with the effects of closure accounted for by a dynamically changing porosity. The pressures in Figure PORSURF-4 are pressures calculated by SANTOS, as outlined above. However, the porosities in Figure PORSURF-3 are the porosities used in BRAGFLO and are obtained from the true porosities calculated by SANTOS by correcting for the repository closure. Specifically,

$$\phi_S V_S = \phi_B V_B ,$$

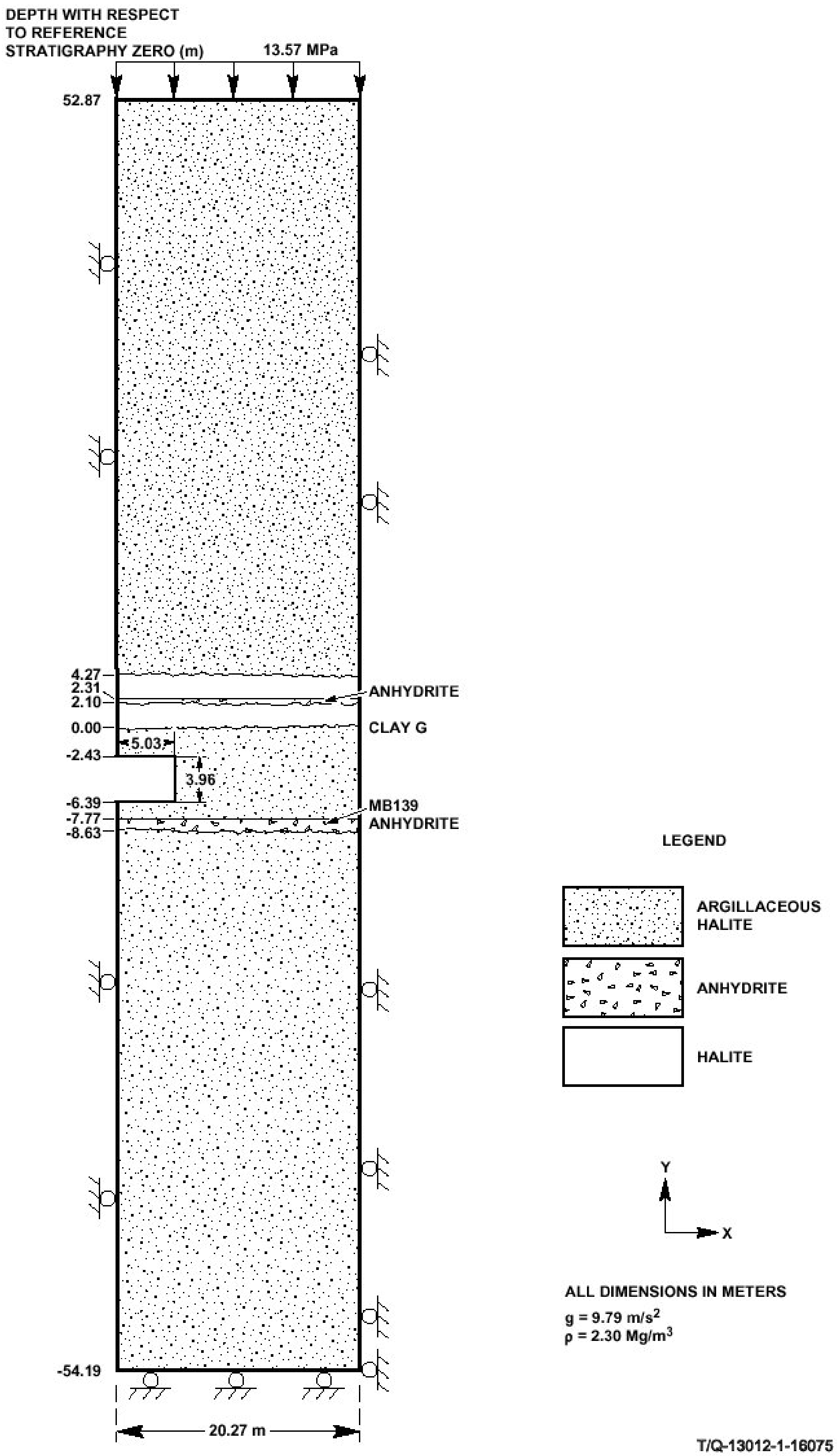

Figure PORSURF-1. Stratigraphy for the Porosity Surface Calculations.

1 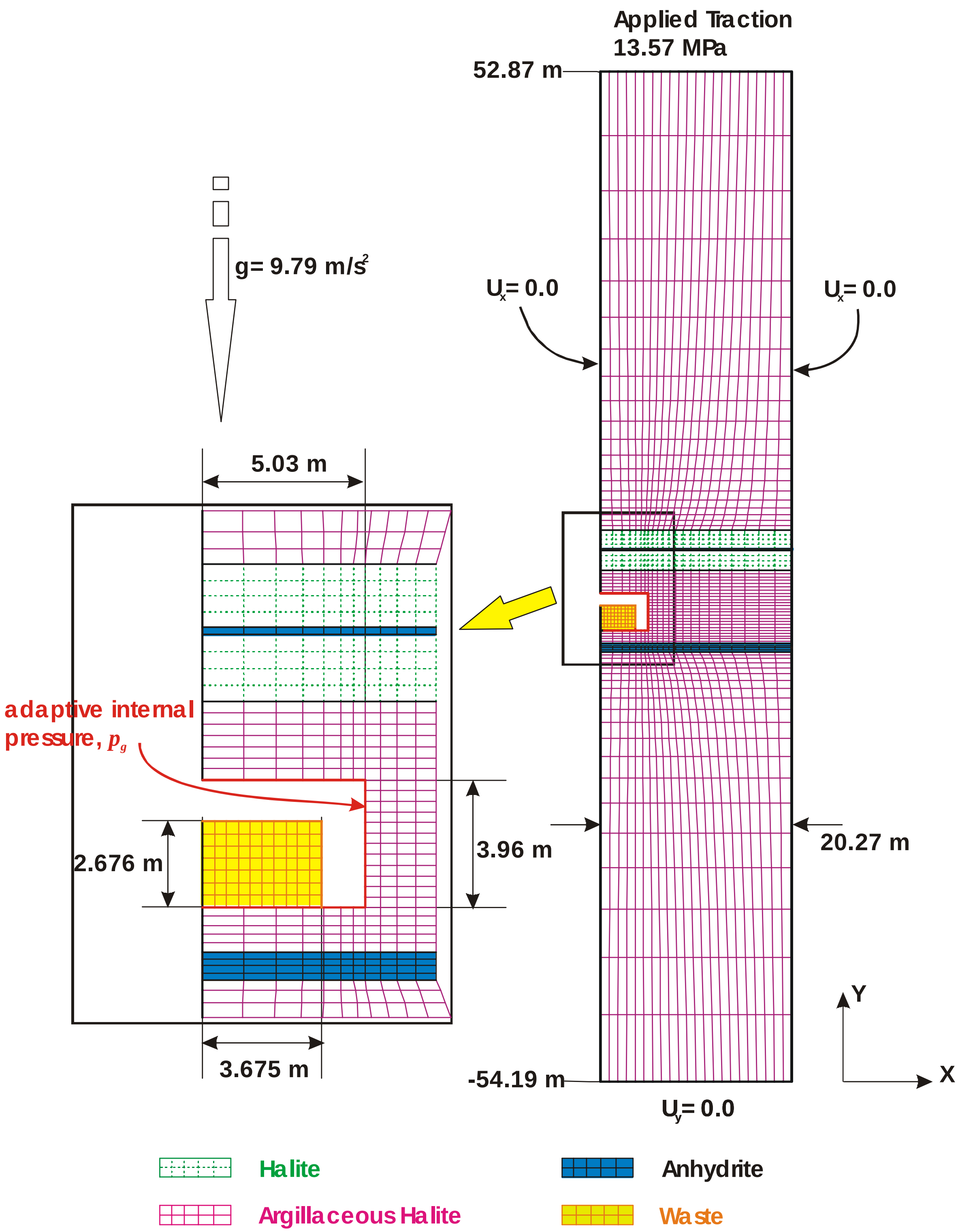

2 **Figure PORSURF-2. Mesh Discretization and Boundary Conditions used for the Porosity**
3 **Surface Calculations.**

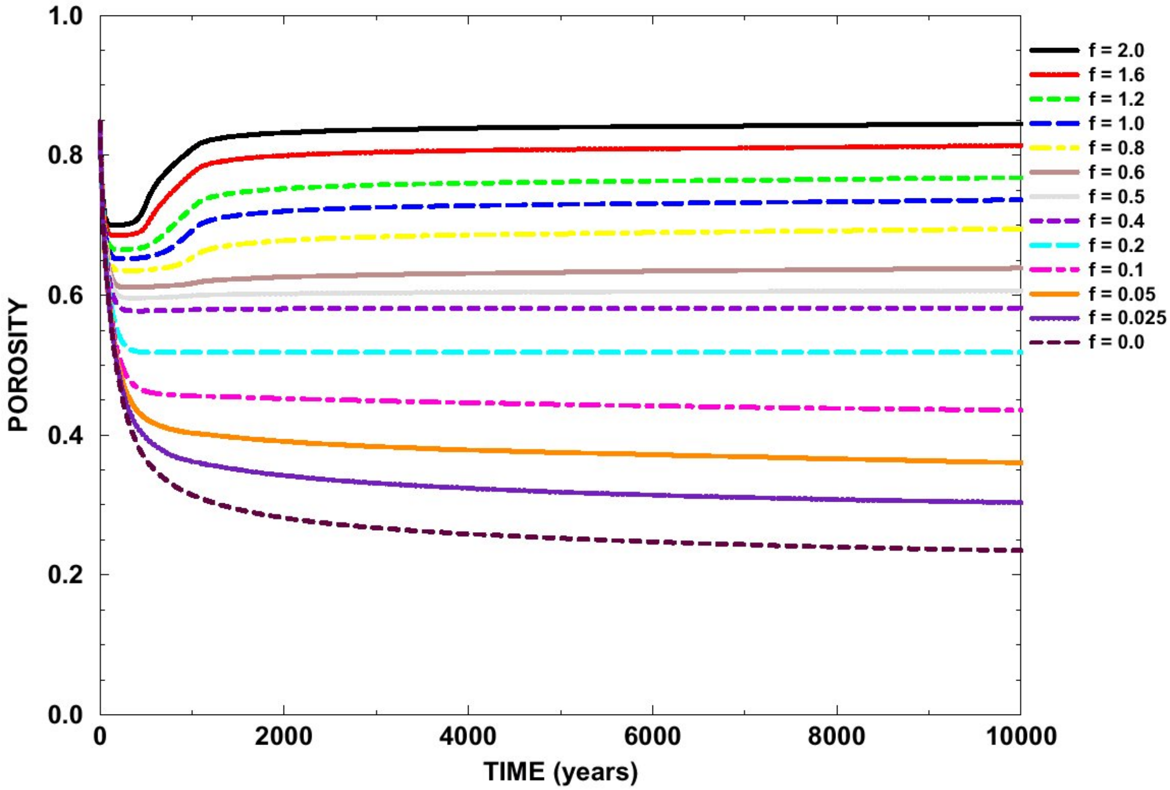

Figure PORSURF-3. Disposal Room Porosity for Various Values of the Scale Factor (f).

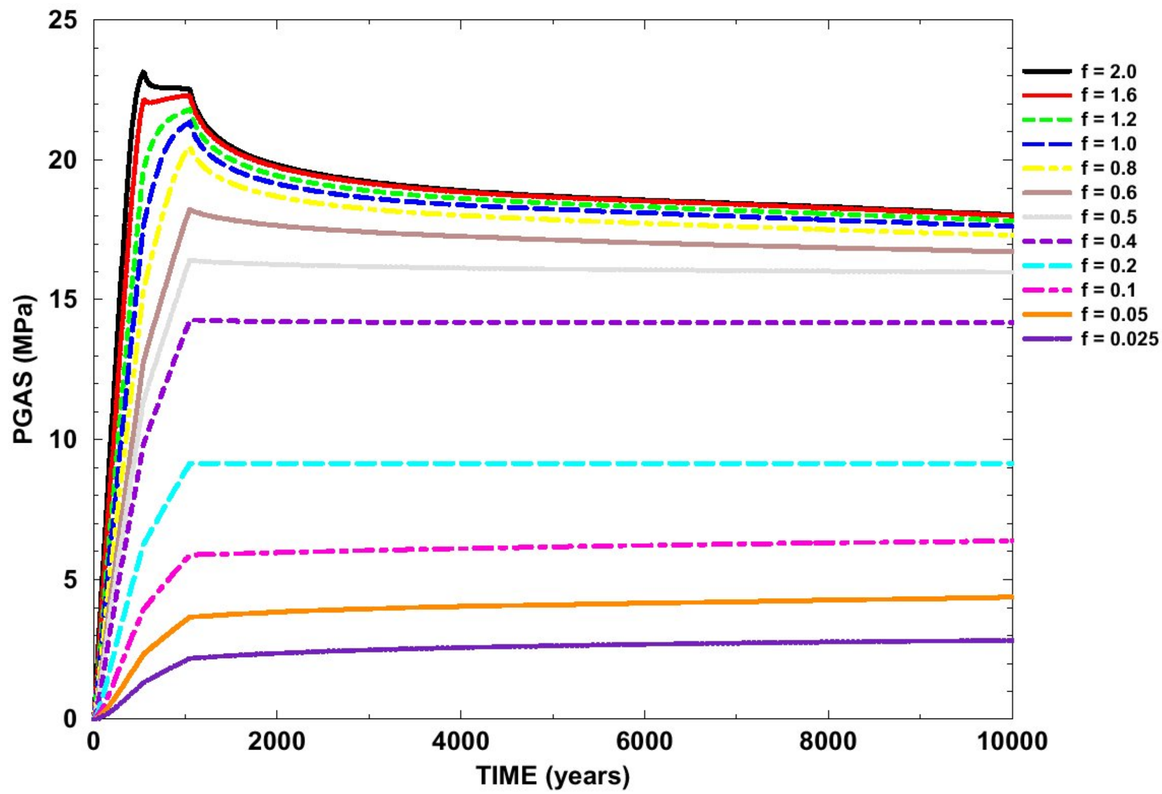

Figure PORSURF-4. Disposal Room Pressure for Various Values of the Scale Factor (f).

where ϕ_S and ϕ_B are the porosities associated with SANTOS and BRAGFLO and V_S and V_B are the total volume per excavated room as represented in SANTOS and BRAGFLO. Note that while V_S changes with time, V_B does not. This formulation conserves the total pore volume in the waste areas between SANTOS and BRAGFLO calculations.

Brine pressures $p_b(t)$ obtained in the waste disposal regions are used in conjunction with the results in Figures PORSURF-3 and PORSURF-4 to estimate porosity in the waste-filled regions for the BRAGFLO calculations. Given a value for $p_b(t)$, values f_1 and f_2 are determined such that

$$p(t, f_1) \le p_b(t) < p(t, f_2),$$

where $p(t, f_i)$ denotes the pressure (Pa) at time t obtained with gas generation rate $r_{f_i}(t)$. An f value associated with $p_b(t)$ is then given by

$$\hat{f} = f_1 + \left(\frac{p_b(t) - p(t, f_1)}{p(t, f_2) - p(t, f_1)} \right) (f_2 - f_1),$$

with $\hat{f}$ being estimated by linear interpolation on f_1 and f_2. With $\hat{f}$ determined, a corresponding porosity $\hat{\phi}$ for use with $p_b(t)$ is obtained from the porosity results in Figure PORSURF-3. Specifically,

$$\hat{\phi} = \phi(t, f_1) + \left(\frac{\hat{f} - f_1}{f_2 - f_1} \right) \left(\phi(t, f_2) - \phi(t, f_1) \right),$$

where $\phi(t, f_i)$ denotes the porosity at time t obtained with gas generation rate $r_{f_i}(t)$.

PORSURF.6 DYNAMIC CLOSURE OF THE NORTH-END AND HALLWAYS

The porosity surface method is not used to model the north end of the repository occupied by the experimental and operational regions. During development of the CCA PA, a supporting analysis compared brine and gas flow results for two models for closure of the north end of the repository: a dynamic closure model, and a baseline model, in which the porosity and permeability of these regions were held constant (Vaughn et al. 1995). The study examined the effect of these two approaches on brine releases to the accessible environment for both disturbed and undisturbed conditions, as well the effects on brine pressures and brine saturations in the modeled regions. The study concluded that the baseline case (assuming constant low porosity and high permeability) consistently led to either similar or more conservative brine pressures and brine saturations, thereby overestimating potential releases relative to the dynamic consolidation case. Consequently, PA uses the simplifying case of constant porosity and permeability in the northern end of the repository, rather than modeling dynamic closure of these areas.

PORSURF.7 ADDITIONAL INFORMATION

The following attachments were included in CCA Appendix PORSURF to document additional details of the porosity surface method:

1. Attachment 1 to Appendix PORSURF of the CCA, Proposed Model for the Final Porosity Surface Calculations. This memo documents preliminary configuration and constitutive property values for the final porosity surface calculations. Tables in the memo include elastic and creep properties for clean halite and argillaceous halite, volumetric strain data and material constants used in the volumetric-plasticity model for waste, and elastic and Drucker-Prager constants assigned to anhydrite Marker Bed 139. This attachment was supplemented and updated subsequent to the CCA by Butcher (1997a; 1997b).

2. Attachment 2 to Appendix PORSURF of the CCA, Baseline Inventory Assumptions for the Final Porosity Surface Calculations. This memo discusses the effect of changes in the Transuranic Waste Baseline Inventory Report (TWBIR) on the SANTOS analyses.

3. Attachment 3 to Appendix PORSURF of the CCA, Corrosion and Microbial Gas Generation Potentials. This memo discusses the rationale for the base gas production potentials of 1,050 moles/drum for corrosion and 550 moles/drum for microbial decay in the SANTOS analyses.

4. Attachment 4 to Appendix PORSURF of the CCA, Resolution of Remaining Issues for the Final Disposal Room Calculations. This memo provides additional detail on the disposal room elevation, determination of plastic constants for transuranic (TRU) waste, and determination of SANTOS input constants for clean halite, argillaceous halite, and anhydrite.

5. Attachment 5 to Appendix PORSURF of the CCA, Sample SANTOS Input File for Disposal Room Analysis. A representative sample input file is provided in this attachment. The only difference between this input file and the file used in the CCA calculations (see Stone 1997) is a subroutine modifying the gas generation variable.

6. Attachment 6 to Appendix PORSURF of the CCA, Final Porosity Surface Data. This attachment provides SANTOS results for selected gas generation scaling factors f = 2.0, f = 1.0, and f = 0.5. This attachment was updated and published as a formal SAND report (Stone 1997) subsequent to submittal of the CCA.

7. Attachment 7 to Appendix PORSURF of the CCA, SANTOS - A Two-Dimensional Finite Element Program for the Quasistatic, Large Deformation, Inelastic Response of Solids. This report provides documentation on the SANTOS code.

REFERENCES

Butcher, B.M. 1997a. Waste Isolation Pilot Plant Disposal Room Model. SAND97-0794. Albuquerque, NM: Sandia National Laboratories.

Butcher, B.M. 1997b. A Summary of the Sources of Input Parameter Values for the Waste Isolation Pilot Plant Final Porosity Surface Calculations. SAND97-0796. Albuquerque, NM: Sandia National Laboratories.

Stone, C.M. 1997. Final Disposal Room Structural Response Calculations. SAND97-0795. Albuquerque, NM: Sandia National Laboratories.

Freeze, G.A. 1996. Repository Closure - Reasoned Argument for FEP Issue DR12. Sandia National Laboratories, Albuquerque, NM.

Freeze, G.A. Larson, K.W., and Davies, P.B. 1995. Coupled Multiphase Flow and Closure Analysis of Repository Response to Waste-Generated Gas at the Waste Isolation Pilot Plant (WIPP). SAND93-1986. Sandia National Laboratories, Albuquerque, NM.

Vaughn, P. Lord, M., and MacKinnon, B. 1995. ADR-3 Dynamic Closure of the North-End Hallways. Summary Memorandum of Record to D.R. Anderson, September 28, 1995. SWCF-A: 1.1.6.3. Sandia National Laboratories, Albuquerque, NM.

U.S. DOE (U.S. Department of Energy). 1996. Title 40 CFR Part 191 Compliance Certification Application for the Waste Isolation Pilot Plant. DOE/CAO-1996-2184. Carlsbad, NM: U.S. Department of Energy, Waste Isolation Pilot Plant, Carlsbad Area Office.